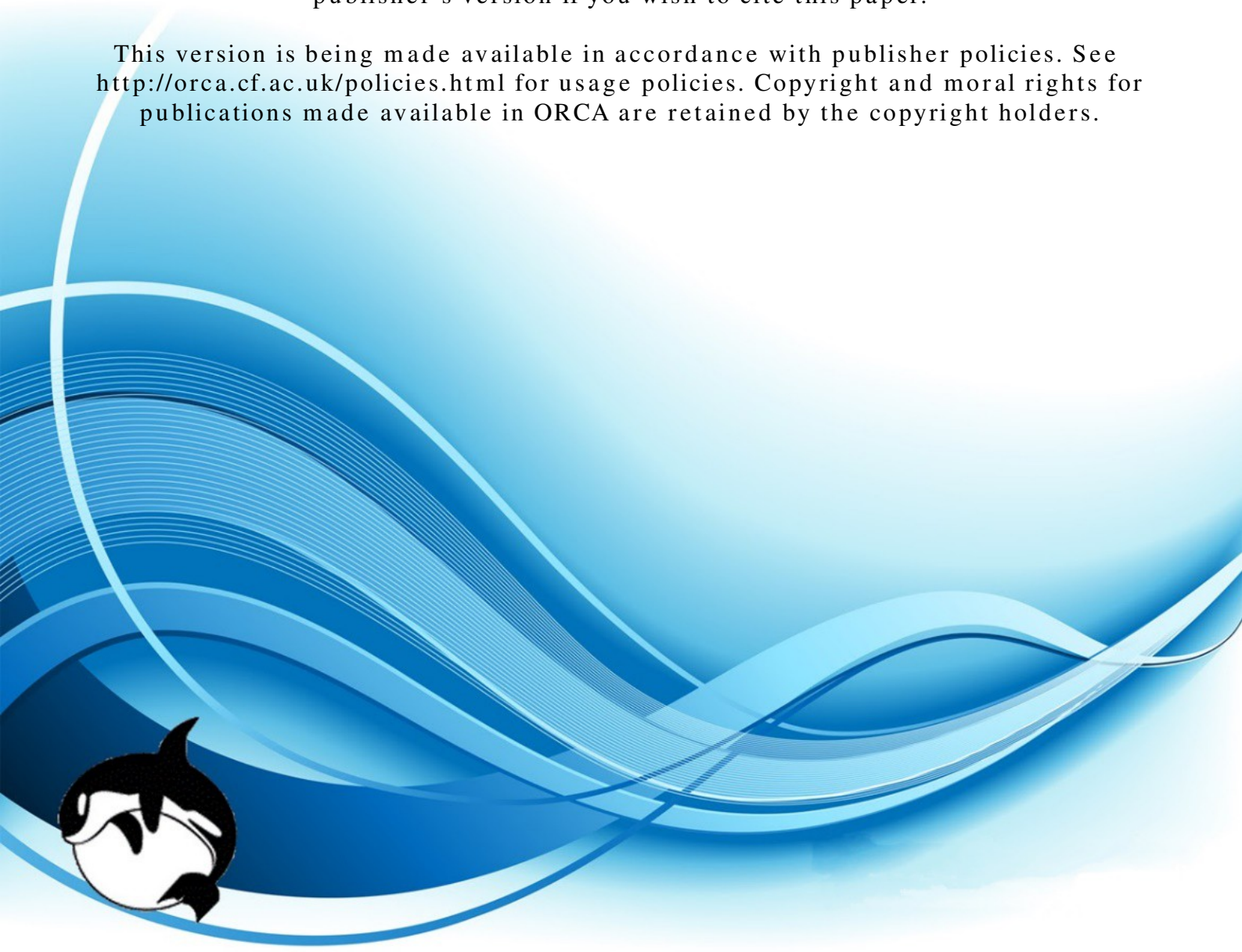

OPPORTUNITIES TO IMPROVE THE UTILISATION OF GRANULATED COALS FOR BLAST FURNACE INJECTION

Julian M Steer[1], Richard Marsh[1], Mark Greenslade[2] Andrew Robinson[3]

1 Cardiff School of Engineering, Cardiff University, Queen's Buildings, The Parade, Cardiff, CF24 3AA, United Kingdom, SteerJ1@cardiff.ac.uk, Tel. +4429 20870599, Fax. +4429 20874939

2 Tata steel UK, Port Talbot, United Kingdom

3 Specific, Baglan Bay Innovation & Knowledge Centre, Central Avenue, Baglan, Port Talbot, SA12 7AX

ABSTRACT

Coal injection plays an important role to the economic success of ironmaking by substituting a portion of the coke input and improving the blast furnace productivity. Manufacturers are looking at opportunities to increase their coal selection options by using higher proportions of technically challenging lower volatile matter content coals; this paper investigates the kinetics, devolatilisation and burnout of these in granulated coal blends using thermogravimetric analysis (TGA) and a drop tube furnace (DTF).

The char residue from the semi-anthracitic low volatile coal selected for this blending investigation had a much reduced reactivity at higher conversions which affected the blends in different ways. Burnout of the blends with the low volatile bituminous coals was improved by fragmentation of the granulated particles, but at longer residence times the lower reactivity of the more structurally ordered carbon in the semi anthracitic coal dominated. In contrast, the higher volatile coals showed improvements at low residence times corresponding to rapid volatile loss, but also showed non-additive blend improvement at longer residence times which may be explained by the more obvious presence of included minerals and the higher K/Al ratios associated with illite mineral phases known to improve burnout.

Keywords: Blast furnace; granulated coal injection; combustion; devolatilisation; blends.

1. INTRODUCTION

Coal injection in the blast furnace is understood to reduce the consumption of expensive coking coals, increase productivity, increase flexibility in operation, improve the consistency of hot metal quality, and reduce the overall emissions from steel plants [1]. Typically, coal is injected into the blast line at temperatures around 1100°C, and the particle residence time in the 'raceway' void formed by this hot blast is typically around 30 to 50 ms [2]; however, Guo et al described work showing how raceway residence times could range from 25 to 1000ms depending on the particle size due to turbulent conditions experienced in this region [3].

In most cases, coal is injected in a pulverised form where the particle size is typically below 75µm; but this paper looks at granulated coal injection, which involves less energy to mill into specification, with a nominal sieve specification of 100% <1000 µm and 50% <250 µm [4, 5]. However, the wider range and larger particle sizes are known to affect the devolatilisation and combustion of coals to a lesser or greater extent due to reasons such as heat transfer, mass diffusion, reactive surface area available, and maceral or mineral segregation affects [6-9] .

Variability in coal properties can influence the quality of the hot metal, furnace stability, productivity and the off gas composition. Because of the short residence time in the raceway the devolatilisation and combustion of coal particles are vitally important, because unburnt particulates indicate un-utilised coal which increases the carbon input per tonne of hot metal and can interfere with the permeability of the furnace [10-12]. For this reason the volatile content, or fuel ratio (fixed carbon/volatile matter), is often used by manufacturers as a measure of the suitability of a coal for injection and consists of combustible gases, incombustible gases, and condensable tars [13, 14].

Higher volatiles generally have better combustion efficiency and produce more reactive chars and hence better burnout [15]. In comparison, low volatile coals with higher calorific values give better coke replacement ratios with less raceway cooling, but usually have lower combustion efficiency leading to unburnt chars [16, 17]. However, higher volatile matter content coal can produce more soot which has lower reactivity than unburnt chars [18].

In order to utilise the optimum properties of both volatile scenarios, coals are often blended, but mixing has been found to alter the combustion properties depending on the coals chosen [16, 19]. Kunitomo et al., found that high volatile matter coal formed a higher temperature combustion field that promoted the combustion of low volatile coals [20] whereas when Artos et al blended high and low-rank coals they found it did not affect the combustion behaviour of the component coals when investigated in a thermogravimetric analyser or drop tube furnace [21]. However, there is also potential for individual coals to cause specific issues with grindability, combust at different rates and temperatures, and burnout at varying rates [18]. Recently Moon et al., showed non-additive behaviour between parent coals and their blends as the volatile matter content of the low rank coal (higher VM) influences the ignition temperature in the blend, whereas the char of the high rank coal (lower VM) in the blend influences the burnout temperature in the high temperature region [17].

Particularly important for the combustion of lower volatile content coals is the char reactivity and this has been studied in great depth [22-24]. The combustion of char is predominately controlled by chemical reactivity and pore diffusion of reactive and non-reactive gases in and out of the char [25-28]. The mineral content of coals, and the association of this in the coal, has also been shown to have an influencing effect on the devolatilisation and combustion giving effects that range from synergistic, catalytic or inhibitory depending on their levels and composition [29-34].

Although high volatile coals are often chosen for coal injection because of the concerns mentioned previously, more recently there has been a trend to utilise higher proportions of low volatile coals. However, increasing the proportion of these has the potential to reduce the furnace operation stability and increase top gas particulate emissions [1, 18, 35, 36].

This paper measures the reactivity and burnout of coal blends with the more challenging high rank low volatile coals, aiming to establish the reasons how and why they affect the performance. In comparison to the state of the art, this work looks more closely at the use of granulated coals for blast furnace injection, instead of the pulverised coals more extensively covered by the literature for this application; it focuses on the novel way these coals and their blends fragment, swell and act synergistically on the burnout in a drop tube furnace.

2. MATERIALS AND METHODS

2.1 Materials

Five coals, ranging from the high rank semi-anthracitic LV1 to the lower rank high volatile bituminous HV, were chosen based on their variation in volatile matter shown in Table 1. The low volatile samples LV1, LV2 & LV3 ranged from 8.2 to 14.7% while the medium volatile MV was 24.6% and the high volatile HV up to 32.5%. For the investigation into coal blending, a 'reference' particle size specification was chosen, typical of a granulated coal specification for blast furnace injection, 100% ≤1000 µm with 50% ≤250 µm. The samples were milled to this specification using a TEMA™ disc mill and classified by dry sieving using the standard BS1016-109:1995. Because high rank semi-anthracitic coals can lead to unburnt particulates when injected into a blast furnace manufacturers are limited to how much they can incorporate, so for this research blends with 40 wt% LV1 were used.

Table 1 Analyses of coals (dried).

	Proximate analyses				**Petrographic analyses**			
Coal type	**Volatile matter content** (% wt)	**Ash content** (% wt)	**Fixed carbon content** (% wt)	**Gross Calorific value** (MJ/kg)	**Vitrinite** (% vol)	**Liptinite** (% vol)	**Inertinite** (% vol)	**Mineral matter** (% vol)
LV1	8.2	5.1	86.7	34.4	83	1	14	2
LV2	13.3	8.1	78.6	32.3	60	0	39	1
LV3	14.7	4.3	81.0	34.4	78	1	18	3
MV	24.6	8.1	67.3	31.3	52	1	46	1
HV	32.5	7.0	60.5	32.3	71	10	17	2

The coal ash from each of the samples was analysed to identify the constituent elements and their variation, shown in

Table 2, represented as the most stable oxide form.

Table 2. Inductively coupled plasma analysis of coal sample ash (% wt)

	Al_2O_3	Fe_2O_3	CaO	ZnO	TiO_2	MgO	CuO	Na_2O	P_4O_5	SiO_2	K_2O	Total
LV1	25.0	7.6	2.6	0.0	0.9	0.8	0.1	0.7	1.3	40.1	1.9	81.0
LV2	26.1	6.1	2.1	0.0	1.8	0.8	0.0	0.9	0.8	42.5	1.4	82.5
LV3	29.0	8.3	2.1	0.0	0.7	1.4	0.0	1.0	0.8	40.8	1.9	86.1
MV	19.7	6.9	2.1	0.0	0.8	1.0	0.0	0.5	0.3	55.9	2.2	89.4
HV	25.3	4.6	1.6	0.0	1.5	0.6	0.0	0.5	0.1	49.5	1.7	85.5

2.2 Methods

2.2.1 Proximate and Petrographic analysis

The classified samples were dried at 105°C using BS11722:2013 until a constant weight and the volatile matter content was measured using standard BS15148:2005. Ash contents were carried out using the standard method BS 1171:2010.

The petrographic maceral analysis was carried out in accordance with ISO7404 by preparing a polished particulate block and carrying out a point count under reflected light microscopy to identify the different macerals present.

A Perkin Elmer Optima 2100D inductively coupled plasma spectrophotometer (ICP–OES) was used to determine the analysis of metal in the coal ash. Samples were prepared for analysis by microwave digestion using aqua regia (1 part HNO_3, 3 parts HCl), followed by hydrofluoric acid (HF, 48%) and boric acid (H_3BO_3).

TGA was carried out using a Perkin Elmer Pyris 1 TGA with an air flow rate or 30ml/min at 4 different heating rates 5, 10, 15 & 20 °C/min. Kinetic analysis of the TGA mass loss and derivative data was used to determine the activation energy by standard BS ISO 11358-2:2005. Ozawa, and later, Flynn and Wall derived the

relationship in Equation 1, where E_a is the activation energy (kJ mol^{-1}) and R is the gas constant which for the four different heating rates and temperatures becomes Equation 2 for a given degree of conversion.

$$\log\beta + 0.4567(E_a/RT) = \text{constant}$$

Equation 1. Ozawa, Flynn and Wall model free kinetic relationship

$$\text{Log}\beta_1 + 0.4567(E_a/RT_1) = \log\beta_2 + 0.4567(E_a/RT_2) = \log\beta_3 + 0.4567(E_a/RT_3) = \log\beta_4 + 0.4567(E_a/RT_4)$$

Equation 2. Ozawa, Flynn and Wall iso-conversional relationship

By plotting the logarithm of the heating rate, logβ, against the reciprocal of the absolute temperature, T^{-1}, for each degree of conversion, α, a series of straight lines were plotted from which the activation energy, Ea, was calculated from the slope ($-0.4567E_a/R$) [37, 38]. The measured activation energy quoted in Table 3 was obtained from the average activation energy for each degree of conversion plot.

Scanning electron microscope (SEM) images were obtained using a FEI SEM-EDX instrument XL30 ESEM FEG at 512x384 resolution in back scattered and secondary electron detection modes.

Particle size analysis work was carried out using a Malvern Mastersizer 3000 laser diffraction particle analyser using a wet cell accessory with obscuration levels between 4-8%.

2.2.2 Devolatilisation and burnout testing using Drop Tube Furnace

A drop tube furnace (DTF) was used to characterise the devolatilisation and burnout behaviour of the coal samples at 1100 °C in air for residence times between 35 ms to 700 ms. The high heating rate and short residence times in the DTF environment closely resemble those experienced when coal is injected into the blast air of the blast furnace raceway making this a particularly relevant technique [12, 18, 24, 39]. Particles were fed into the top at feed rates of 30 g/hr, entrained in a laminar air flow at 20 L/min and collected at the bottom by means of a cyclone collector. The particle residence time was controlled by altering the distance of a moveable water cooled collection probe up to a maximum path length of 1.2 m from a water cooled inlet feeder.

The ash tracer method was used to calculate the burnout of the coals, sometimes referred to as the combustion efficiency [40, 41]. This method assumes that the coal ash remains conserved in the char residue in the test conditions and that no ash species are volatilised. This was tested for all the coal samples at 1100 °C. It is important to note that because the burnout figures are calculated using the ash tracer method, there is room for error propagation which can lead to repeatability issues [42] and the measured standard deviations ranged from 0.2 to 5.2% with an average of 2.6%.

The burnout (%) is calculated from the ash balance of the initial content of ash in the coal (A_0) and the ash content of the residue collected post DTF (A_1).

$$\text{Burnout (\%)} = \frac{10^4(A_1\text{-}A_0)}{A_1(100\text{-}A_0)}$$

Equation 3. Ash tracer burnout

The extent of devolatilisation was determined by measuring the volatile matter content of the residues collected post DTF. These results were then adjusted using the ash tracer method to account for any differences in burnout and to obtain absolute figures for comparison.

3. RESULTS AND DISCUSSION

3.1 Coal blending

To investigate the effects of incorporating lower volatile coals for blast furnace coal injection, four blends were prepared of the HV, MV, LV2 and LV3 coals with 40% of the semi anthracitic low volatile matter content coal LV1. This proportion was chosen as an aspirational target because the injection of these coals in the blast furnace has been shown to be problematic at higher levels [10]. The Thermogravimetric analyser (TGA) was used to compare some of the specific parameters affected by blending because of its suitability to accurately measure thermal mass loss change with controlled heating rates. From this measurement the ignition temperature, peak mass loss temperature and mass loss rates were obtained and the Ozawa- Flynn, iso-conversional, model free, kinetic method used to calculate the activation energy.

In relation to a blast furnace raceway where the heating rates are in the order of 10^4-10^5 ˚C/s [10], the heating rates of a TGA (10°C/min) are orders of magnitude lower with small sample masses (~20mg) and a bulk sample analysis method where there are potential interaction and gas diffusivity effects. However, the technique is fast, reliable and convenient. In contrast to this, the drop tube furnace (DTF) measures burnout and devolatilisation under high particle heating rate conditions (10^4 ˚C/s) [43], dilute particle phase and high temperatures. Because of its similarity to the raceway conditions, this makes the DTF a very useful comparison technique.

3.2 Thermogravimetric (TGA) and kinetic analysis

Thermal analysis profiles of the mass loss versus temperature are shown in Figure 1a for the unblended coals and Figure 1b for the blended coal samples as measured using the TGA at a 10 °C/min ramp rate. The derivative curves plot the rate of mass loss for the coals versus temperature for the unblended coals in Figure 2a and for the blended coals in Figure 2b.

Because of the short particle residence time in the raceway ca. 35ms [2], blast furnace iron manufacturers use the volatile matter loss as an important technical parameter to determine the suitability of coal. With respect to temperature, the mass loss profiles approximately follow the order of volatile matter content from highest to lowest as might be expected HV, MV, LV2, LV3 and LV1. However, it is worth noting that the profile shape of LV2, in Figure 1a, indicates higher char reactivity at high conversion levels with a lower burnout temperature compared to the other lower volatile coals. Although higher volatiles have been shown by some authors to produce more reactive chars [15], this is not always the case, and Australian low volatile coals with similar volatile matter contents have been shown to display different char reactivities, suggesting differences between coals of similar VM [44]. Conversely, the lowest volatile coal LV1 had the broadest derivative curve with the lowest rate of mass loss change suggesting that in addition to a low volatile content this coal had lower char reactivity.

For the coal blends, shown in Figure 2b, the profiles were closer with a narrower band of variation reflecting the smaller volatile blend range of 10.6% – 23.2%, compared to the unblended coals 8.2 % - 32.5 %. As expected because of the higher volatile matter content, the HV and MV blends show mass loss at a lower temperature than the lower volatile blends of LV2 and LV3. However, although the unblended LV2 coal had a mass loss profile at a lower temperature relative to the other low volatile coals, the profile for the blended

LV2 showed a negative effect with the incorporation of LV1 coal with mass loss occurring at higher temperatures.

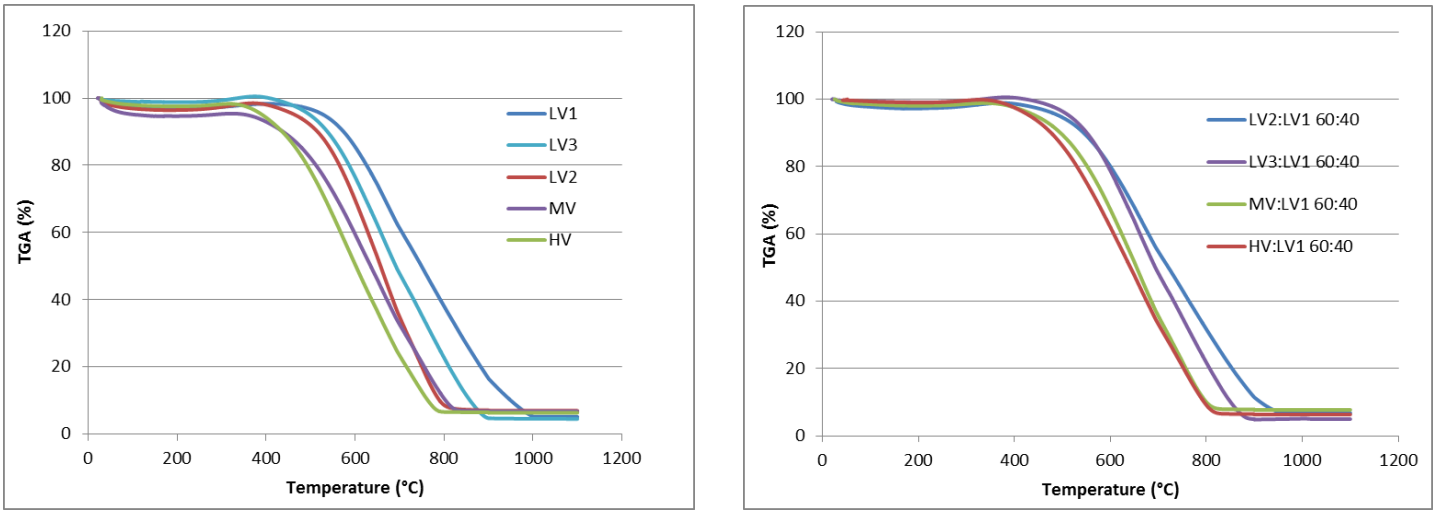

Figure 1. Thermogravimetric mass loss curves for a) unblended and b) blended coals at 10°C/min heating rate

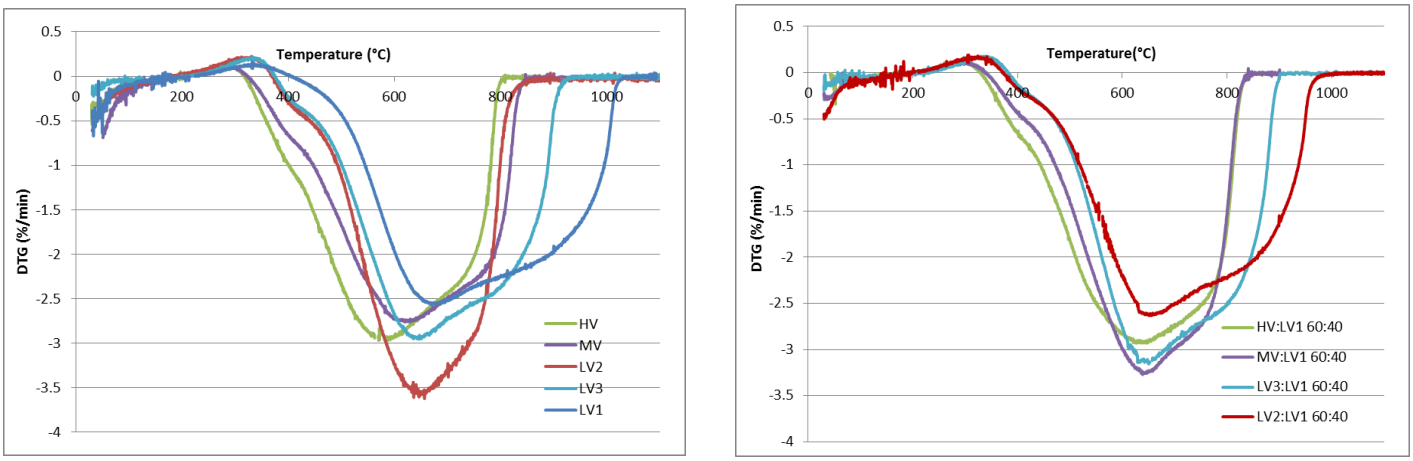

Figure 2. Derivative thermogravimetric rate of mass loss curves for a) unblended and b) blended coals

The quantitative measured figures for the unblended coals shown in Table 3 show a generally decreasing trend of lower ignition temperature, peak temperatures, burnout temperatures, and activation energy associated with higher volatile contents. To compare the effect of blending, the theoretical values for the different parameters were calculated from the measured figures for the unblended coals assuming simple proportional additive behaviour.

A combustibility index was used to compare the different parameters together and incorporates the mass loss and the derivative mass loss; the higher this figure, the better the overall combustibility. The index is defined

in Equation 4 and is made up of the maximum rate of weight loss (dw/dt)max, the average rate of weight loss (dw/dt)mean, the ignition temperature (T_i) and burnout temperature (T_b) [45].

$$S = \frac{(dw/dt)\,mean\ \ (dw/dt)\,max}{Ti^2\ Tb}$$

Equation 4. Combustibility index

The lowest VM LV1 coal had a significantly lower reaction index (0.9) compared to the other unblended coals, but although their VM contents were quite different (Δ = 19.2%), the combustibility index of the LV2 coal and the HV were close (1.99 and 2.08) due to the faster combustion rate of the LV2 char. In addition to the benefit of blending coals with better combustibility properties, the process of blending showed both synergistic and inhibitory non-additive blending results.

Compared to the theoretical values the ignition temperature, peak temperature and to a lesser extent the burnout temperature exhibited additive behaviour on blending. However, there was a marked reduction in the activation energy and a marked increase in the combustibility with the higher volatile coals and particularly with the LV3 coal. Considering the relatively small difference in volatile contents (6.5%) for the LV1 and LV3 this suggests a synergistic effect separate to the VM order. In contrast, the LV1 had an inhibitory effect on the mass loss rates in particular which, when blended with LV2, severely reduced the combustibility index (-36.7%).

Table 3. TGA and kinetic parameters

SAMPLES	LV1	LV2	LV3	MV	HV	LV2:LV1 60:40	LV3:LV1 60:40	MV:LV1 60:40	HV:LV1 60:40
Ignition temperature (°C)	545	492	501	447	400	519	512	472	444
Theoretical value						513	519	486	458
% change compared to theoretical						1.1	-1.3	-2.9	-3.1
Peak Temp (°C)	675	636	637	625	570	631	626	622	621
Theoretical value						652	652	645	612
% change compared to theoretical						-3.2	-4.0	-3.6	1.5
Burnout temp (°C)	1032	861	916	848	806	978	901	843	841
Theoretical value						929	962	922	896
% change compared to theoretical						5.2	-6.4	-8.5	-6.2
Activation energy (E_a)*	86.0	50.3	50.3	38.8	36.3	66.9	42.7	53.7	54.4

(kJ mol^{-1})									
Theoretical value						68.1	68.1	62.4	61.1
% change compared to theoretical						-1.8	-59.5	-16.3	-12.4

Combustibility index (x10^{-8})	0.9	1.99	1.25	1.52	2.08	0.90	1.48	1.65	1.94
Theoretical value						1.56	1.12	1.28	1.61
% change compared to theoretical						-36.7	32.7	29.1	20.0

*Average measurement of different degrees of conversion

Table 4 shows the activation energy and correlation coefficients for the coals and blends at different levels of conversion and describes more specifically what happens when the samples are blended. For the unblended low volatile LV1 the activation energy increases with conversion and indicates the lower reactivity of its char which affects each coal blend differently, this is consistent with increased carbon structure ordering and preferential consumption of less ordered carbon. The crystalline phase of carbon is expected to increase with coal rank which agrees with the order of the unblended samples from the semi anthracitic LV1 to the high volatile bituminous HV which affects the char reactivity [22-24, 28]. However, the TGA blend results showed a non-additive coal specific behaviour for the LV2 blend which measured decreasing char reactivity whereas with the LV3 the char reactivity increased. With the higher volatile coals the LV1 had a negative effect on the devolatilisation but the MV and HV coals improved the char reactivity.

Table 4. Activation energy and correlation coefficients at different levels of mass conversion

	LV1		**LV2**		**LV3**		**MV**		**HV**	
Conversion	R^2	E_a (kJ/mol)	R^2	E_a (kJ/mol)	R^2	E_a (kJ/mol)	R^2	E_a (kJ/mol)	R^2	E_a (kJ/mol)
0.1	0.9127	64.5	0.8495	48.4	0.8866	55.0	0.9260	35.9	0.9903	43.0
0.3	0.9956	81.0	0.8178	53.3	0.8389	52.8	0.9998	44.0	0.9908	38.3
0.5	0.9864	96.7	0.7410	52.1	0.7906	47.4	0.9854	40.7	0.9972	33.9
0.7	0.8837	101.6	0.6580	47.5	0.7552	46.1	0.9459	34.8	0.9999	30.2

	LV2:LV1		**LV3:LV1**		**MV:LV1**		**HV:LV1**	
Conversion	R^2	E_a (kJ/mol)	R^2	E_a (kJ/mol)	R^2	E_a (kJ/mol)	R^2	E_a (kJ/mol)
0.1	0.9972	58.5	0.8694	54.6	0.9274	60.2	1.0000	71.8
0.3	0.9996	68.2	0.8306	46.1	0.9950	57.5	0.9855	54.5
0.5	0.9887	67.6	0.7966	37.6	0.9912	52.4	0.9753	48.4
0.7	0.9718	73.4	0.7465	32.7	0.9350	44.6	0.9636	42.9

3.3 Drop tube furnace

A drop tube furnace (DTF) was used to investigate and compare the burnout of coals in air at 1100°C, a similar temperature to that used for the hot air blast used for coal injection. The high heating rates and dilute particle phase make this equipment and technique very useful because of the similarities with the raceway region of the blast furnace.

The burnouts for the unblended coals shown in Figure 3 closely follow the order of increasing volatile matter content with improving burnouts from LV1 (48.1%) to a much higher HV (86.2%) and similar profile shape. The exception to this pattern was LV3 which exhibited a slightly steeper profile shape at longer residence times. The low volatile coals were all characterised by low burnout (<10%) at low residence times which has particularly important implications for blast furnace injection where residence times in the raceway are low contributing to the challenge of using these coals. However, the higher volatile coals HV and MV both have better burnouts at low residence times because of the volatile matter mass loss.

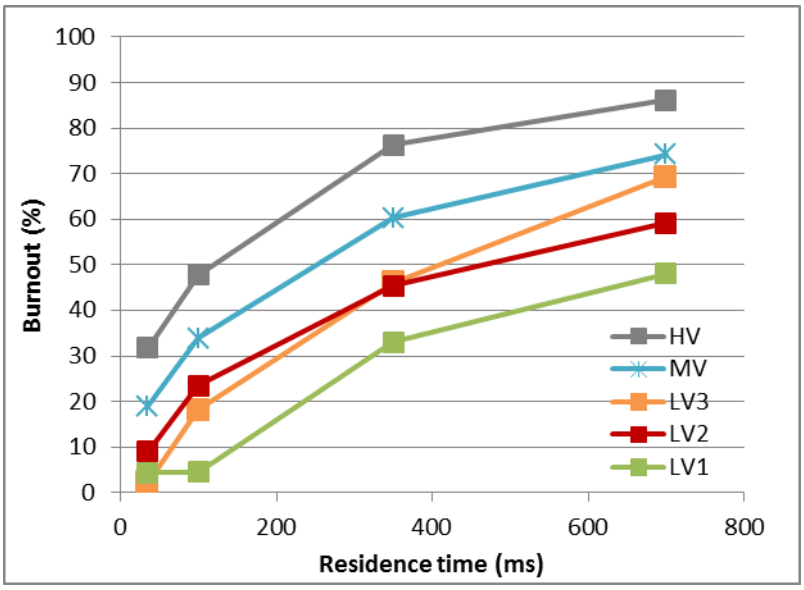

Figure 3. Sample burnout of unblended coals in drop tube furnace at 1100°C

Each of the sample burnouts for the blends with LV1 has been plotted alongside the unblended constituent coals and against the theoretical blend profile assuming additive behaviour to compare the relative effects. Blends with the lower volatile coals LV2 and LV3 in Figure 4 had little effect at residence times of 35ms because the unblended coals perform poorly. However, both showed equivalent or improved burnout relative to theoretical at 100 ms and 350ms but LV1 influenced the blend most at longer residence times

(700ms) with reductions of 6.1% and 7.5% compared to the theoretical values. This is consistent with the TGA kinetic data at higher conversions where there was a measured increase in the activation energy for LV1 from 64.5 kJ/mol at 10% conversion to 101.6 kJ/mol at 70% conversion. The decrease in reaction rate and therefore burnout at higher conversions is affected by the higher activation requirement required for LV1 and suggests that the coal with lower activation energy burnt out first. However, it should be noted that the synergistic effect of the LV3 blend and the inhibitory effect of the LV2 blend measured by the TGA was not replicated in the DTF burnouts. This may in part be due to the lower overall conversion levels measured in the DTF and because of the much higher heating rates affecting the reactivity of the char formed.

In comparison, blending the higher volatile coals MV and HV, shown in Figure 4, had a beneficial effect on the burnouts due to the volatile matter release which was expected to contribute to a higher particle temperature and burnout [20]. The higher volatile coals appear to have a synergistic effect on the burnouts, particularly at the lower residence times, compared to the theoretical profiles.

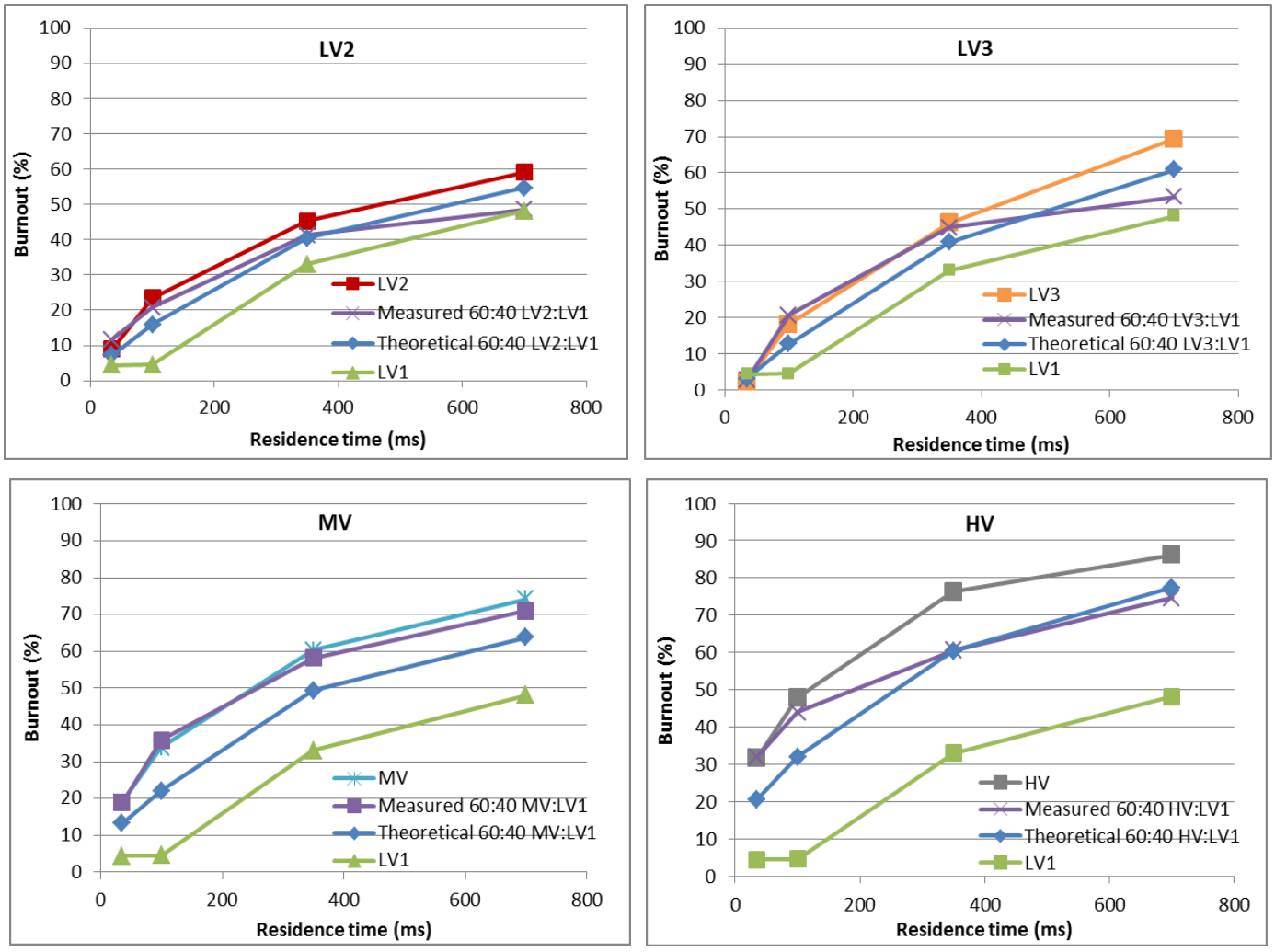

Figure 4. Sample burnouts of unblended and blended coals in drop tube furnace at 1100°C

Because of the measured burnout variation of the blended coals, the devolatilisation has also been plotted to investigate its behaviour. The blend profiles of the LV2, LV3 and MV in Figure 5 showed very little variation compared to the theoretical profiles with no measured synergistic benefit on blending. However, blending the higher volatile content HV, in Figure 5, showed some improvement in the devolatilisation. This effect is believed to be due to an increased particle temperature associated to the rapid burnout of the higher volatile matter content increasing the temperature surrounding the particle, which in turn might be expected to increase the measured volatile yield [20].

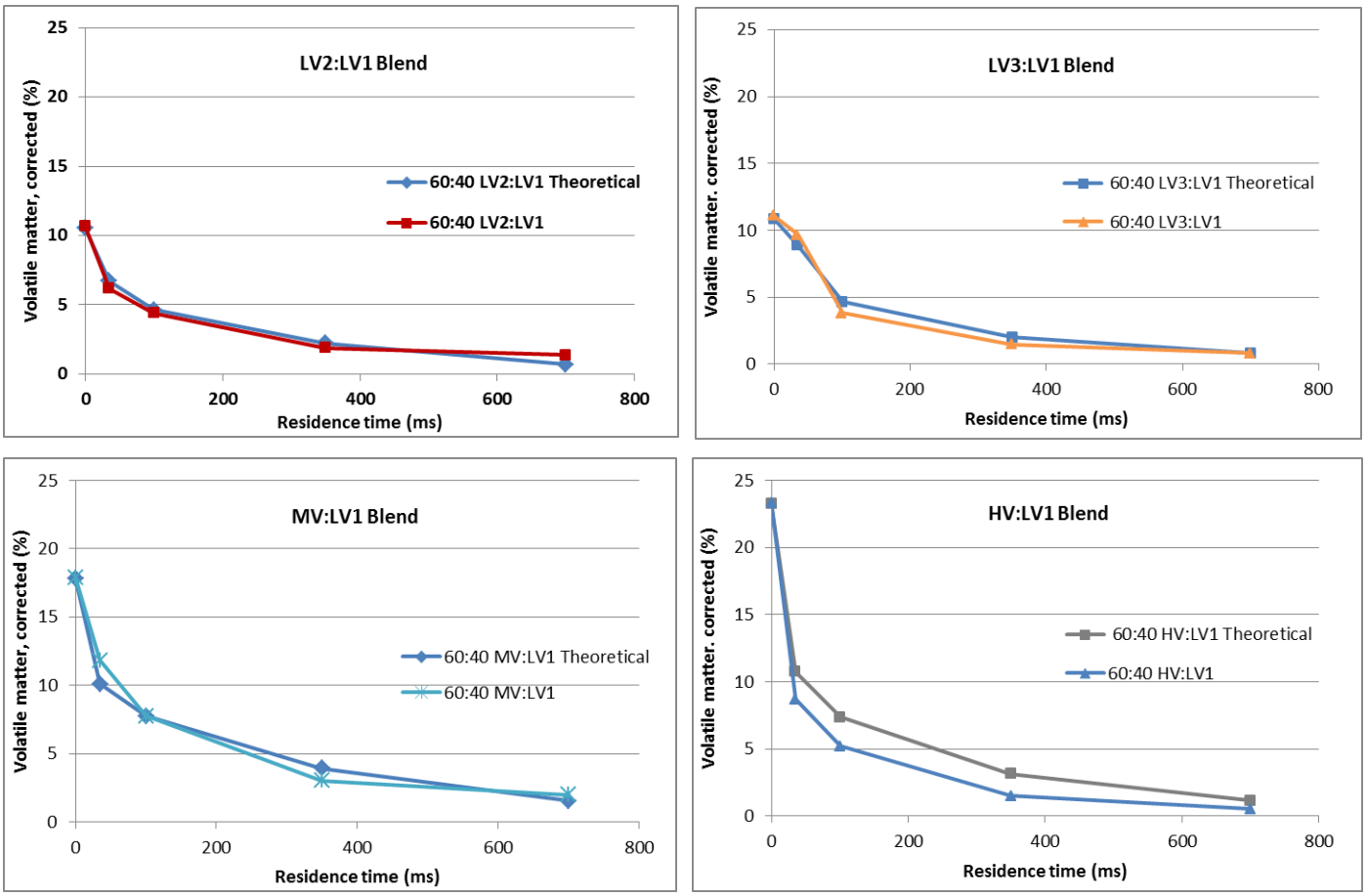

Figure 5. Devolatilisation curves for blends compared to the theoretical profiles

3.4 Particle size analysis

The sample residues after passing through the drop tube furnace at different residence times showed obvious visual changes. Residues after shorter residence times <100ms were characterisatically dark with relatively high levels of unburnt carbon, whereas after longer residence times >350ms the residues become distinctly

lighter with obvious particle swelling. The observations with increasing burnout implied decreasing carbon with reduced density and potentially increased porosity which would affect the reactivity and burnout of the chars formed.

To investigate this more closely, laser diffraction particle size distributions were determined using a Malvern™ Mastersizer 3000. Two distinct effects in the particle size distributions were measured the fragmentation and swelling. The fragmentation occurs where larger particles heat very quickly and break into smaller pieces [46] and would be expected to have a positive effect on the sample burnout as the surface area exposed for reaction increases correspondingly.

Figure 6 shows the difference in the Dv90 (the maximum particle diameter below which 90% of the sample volume exists) sample particle size before and after 35ms in the drop tube furnace. The histogram indicates only a small decrease (50µm) in the Dv90 particle size for the LV1, whereas the other coals all show larger changes particularly with LV2 and LV3 coals with reductions of 554µm and 520µm respectively.

Considering the importance of particle size and surface area with respect to reactivity and burnout, this fragmentation of the particles measured at 35ms could explain why LV2 and LV3 coals measured improved burnout at longer residence times even though the difference in volatile matter content (5.1% and 6.5%) is low. The MV and HV coals also show reductions in the Dv90 (206µm and 241µm) but lower than LV2 and LV3 which could be due to a swelling effect noted in Figure 7 associated with the larger volatile matter content release and offsetting the fragmentation.

For the blended coals there was a measured fragmentation effect at 35ms compared to the LV1, with reductions in Dv90 ranging from 223µm to 462µm compared to the small change of 49µm with the LV1. For the blends with lower volatile matter, the fragmentation could explain the improved burnouts at 100ms and 350ms relative to theoretical, particularly for the LV3 coal blend.

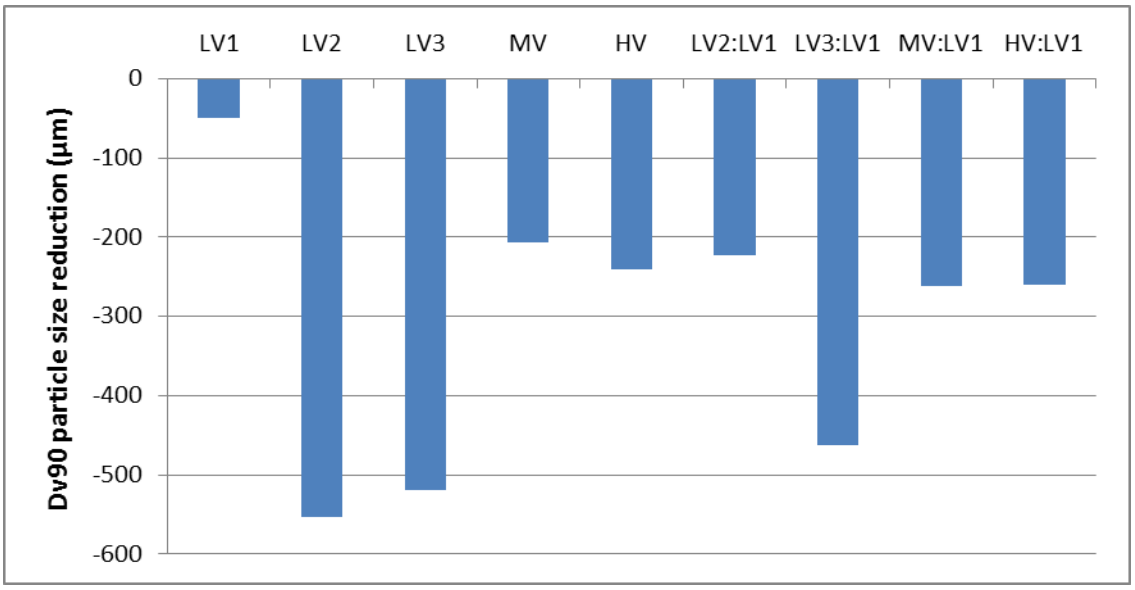

Figure 6. Dv90 particle size reduction after 35ms post DTF compared to initial pre DTF values

The second measured change in particle size distribution was a particle swelling effect which occurred at longer residence times (700ms) in the drop tube furnace, as shown in Figure 7, measured by the Dv90 particle size increase between 35ms and 700ms. An increase in the size of the particles relative to their mass could potentially decrease the density and increase porosity, unless the effect is due to agglomeration.

For the unblended coals, the lowest volatile content LV1 showed little change (-32µm) in the relative Dv90 particle size of the unburnt DTF residues corresponding to the lowest burnout (48%) and consistent with its semi anthracitic rank. However, the other lower volatile content coals, LV2 and LV3, with higher burnouts (59% and 69%), both show relative increases by 375µm and 342µm even though LV3 has a very similar petrographic composition to LV1. The high volatile, MV and HV, both have better DTF burnouts (74% and 86%) and show large relative increases of 755µm and 455µm, caused by the escaping volatile matter and viscoelastic plastic flow of these samples.

For the coal blends with LV1, all the samples measured an increase in the relative particle sizes ranging from 249µm to 364µm. For the lower volatile coals LV2 and LV3, the swelling effect actually corresponded to a reduction in the burnout at 700ms relative to the theoretical values which might suggest agglomeration of the particles reducing the surface area and porosity and consequently affecting the reactivity. For the HV coal blend there was no change in burnout relative to theoretical, but the highest swelling coal MV gave the coal blend with the best burnout profile and the only coal to show improvement at all the residence times.

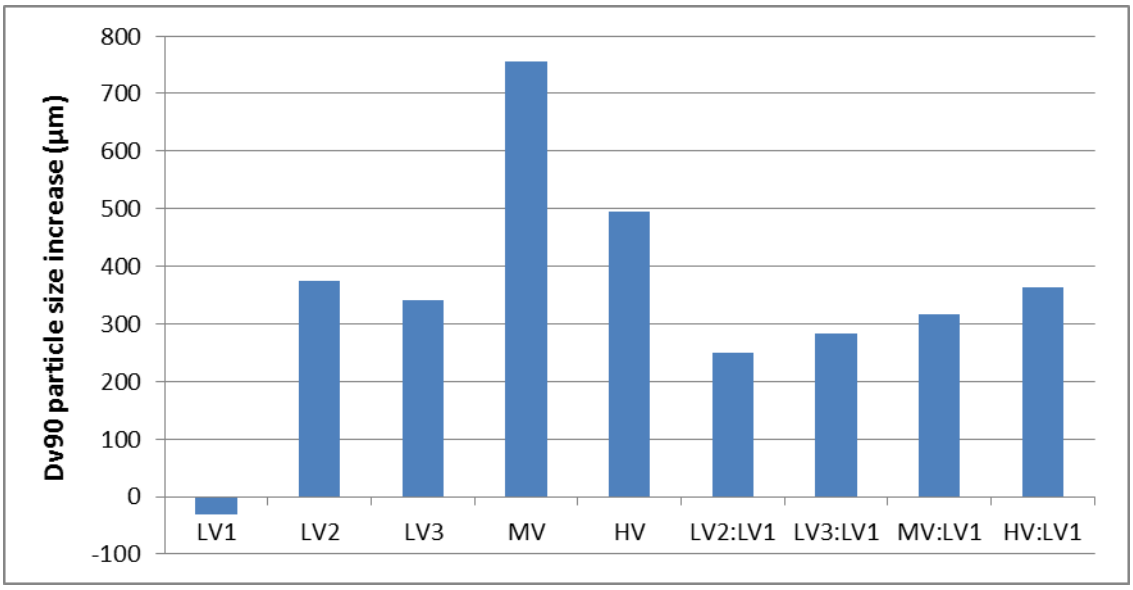

Figure 7. Dv90 particle size increase after 700ms post DTF compared to initial pre DTF values

3.5 SEM Particle analysis

3.5.1 Particle shape and structure post DTF

To investigate the effect of residence time in the DTF on the coal samples, scanning electron microscope images were used to visualise the char forming behaviour of the unblended coals to correlate with blending behaviour. Backscattered electron detection was used to obtain images to look at the fragmentation and compare with the particle effects measured using the Malvern particle size distributions; but it was also selected to highlight the distribution of higher atomic weight elements contributed by the mineral content, because of their potential effect on the reactivity of the samples.

LV1 particles after 35ms in the DTF are shown in Figure 8a and are characterised by sharp edges and brittle fractures from milling, with little evidence of any physical thermal change consistent with the low DTF burnout (4.0%), high TGA activation energy (64.5kJ/mol @ 10% conversion) and low levels of fragmentation measured by laser diffraction. In comparison, in Figure 8b, after 700ms burnout the particles show some surface pores associated with burnout; however, the char formed had the appearance of a solid structure consistent with the semi anthracitic rank with little change in particle shape, suggesting that phases of this coal are very unreactive. This agrees with the much higher char activation energy (101.6 kJ/mol @70%) and lower TGA combustibility index at high conversions and lower DTF burnout after 700ms.

In comparison, the LV2 low volatile coals in Figure 9a and Figure 9b produced cenospherical type char with evidence of explosive fracture, hollow structures with thin walls consistent with the fragmentation observed with the particle size measurement and after 700ms it also showed signs of particle swelling and bubbling. The other low volatile coal LV3 in Figure 10a and Figure 10b also showed characteristics of a cenospherical char structure with thin fractured walls but after 700ms these structures appear to have agglomerated into larger porous chars. These appeared to be bigger than the measured Dv90 figures obtained by laser diffraction which may suggest their hollow nature was more brittle and fracture occurred as the particles were circulated around the diffraction measurement cell.

The images for the MV shown in Figure 11a and Figure 11b appear to show a mixture of thin walled fragments and sintered residues at 35ms and a large swelling effect after 700ms. The char structure appeared to be less open than the LV2 and LV3 with small surface porous holes which might suggest that the higher burnout measured for this coal is more to do with higher reactivity than porosity. In comparison, the HV images shown in Figure 12a and Figure 12b also show the swelling effect, but in difference to the MV, the images after 700ms indicate a more open hollow structure with exposed thin walls and a higher expected porosity correlating with a high burnout 86.2%.

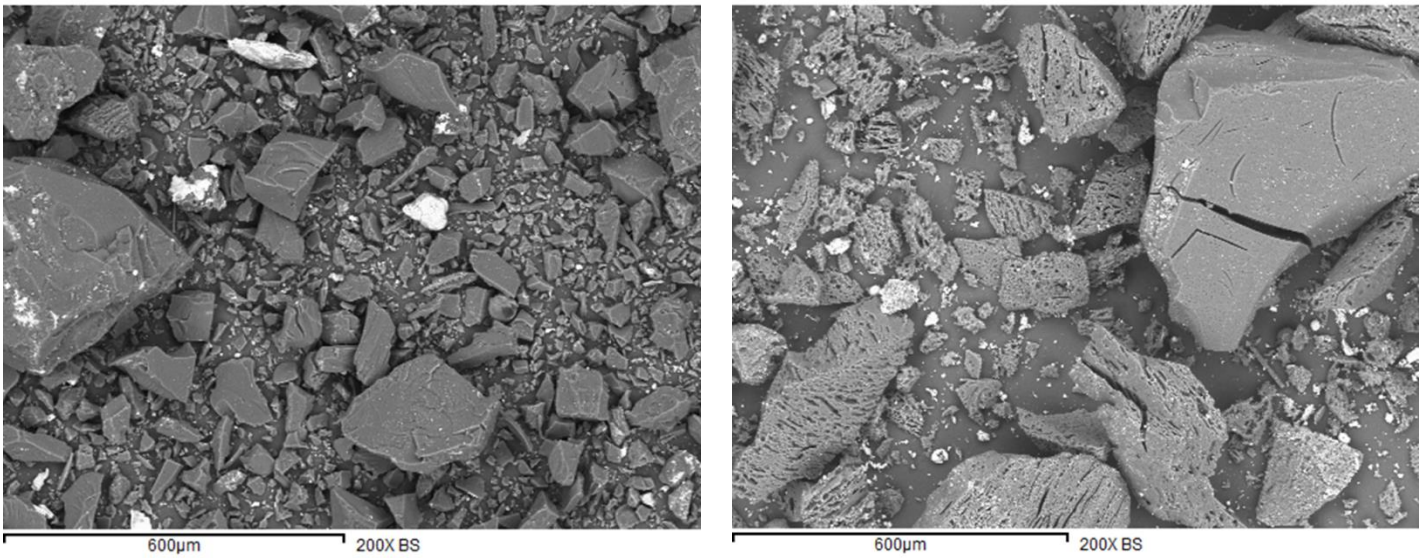

Figure 8. Backscattered images of the DTF residue of LV1 after a) 35ms and b) 700ms

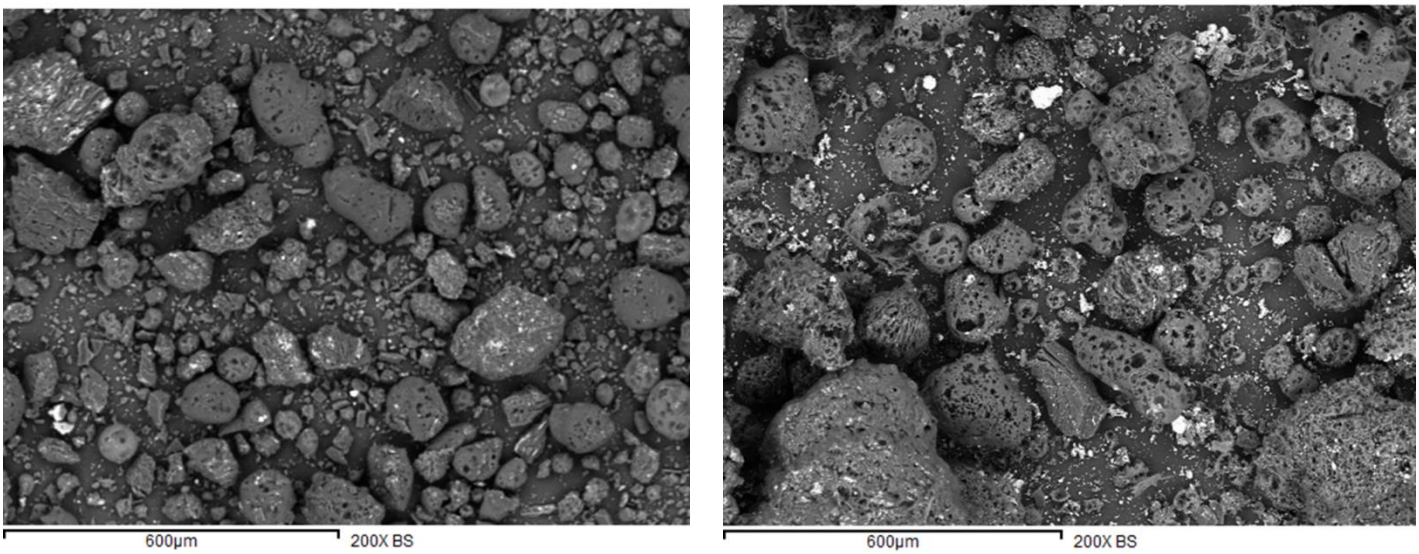

Figure 9. Backscattered images of the DTF residue of LV2 after a) 35ms and b) 700ms

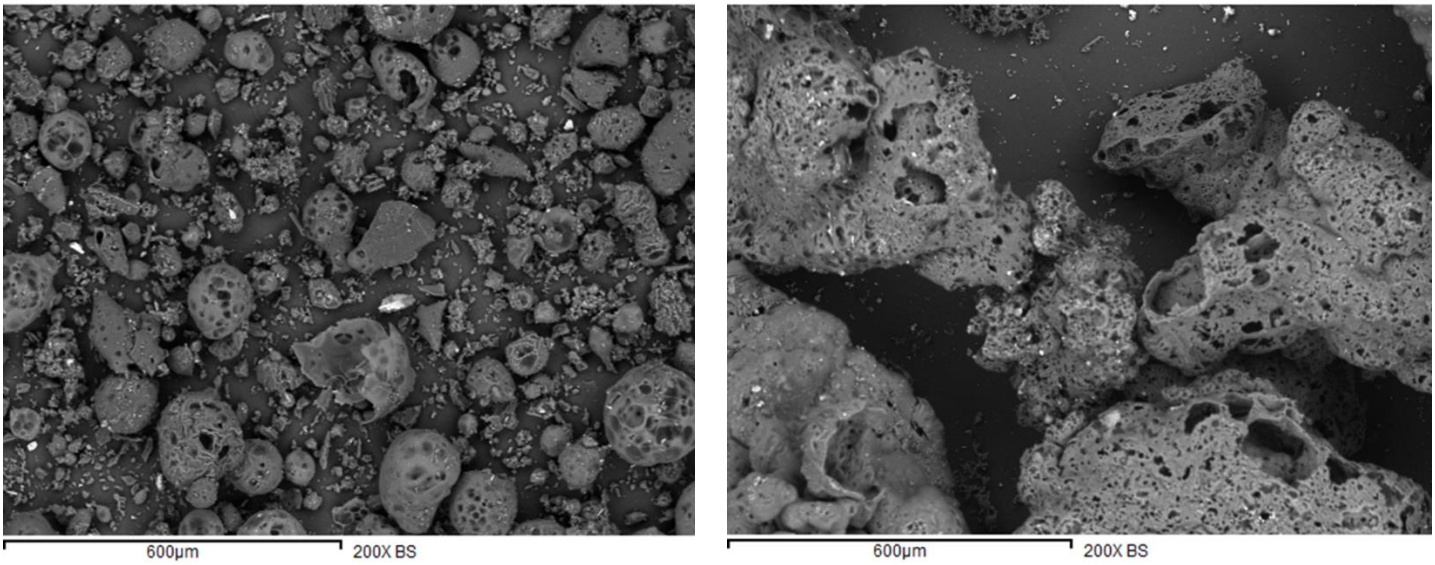

Figure 10. Backscattered images of the DTF residue of LV3 after a) 35ms and b) 700ms

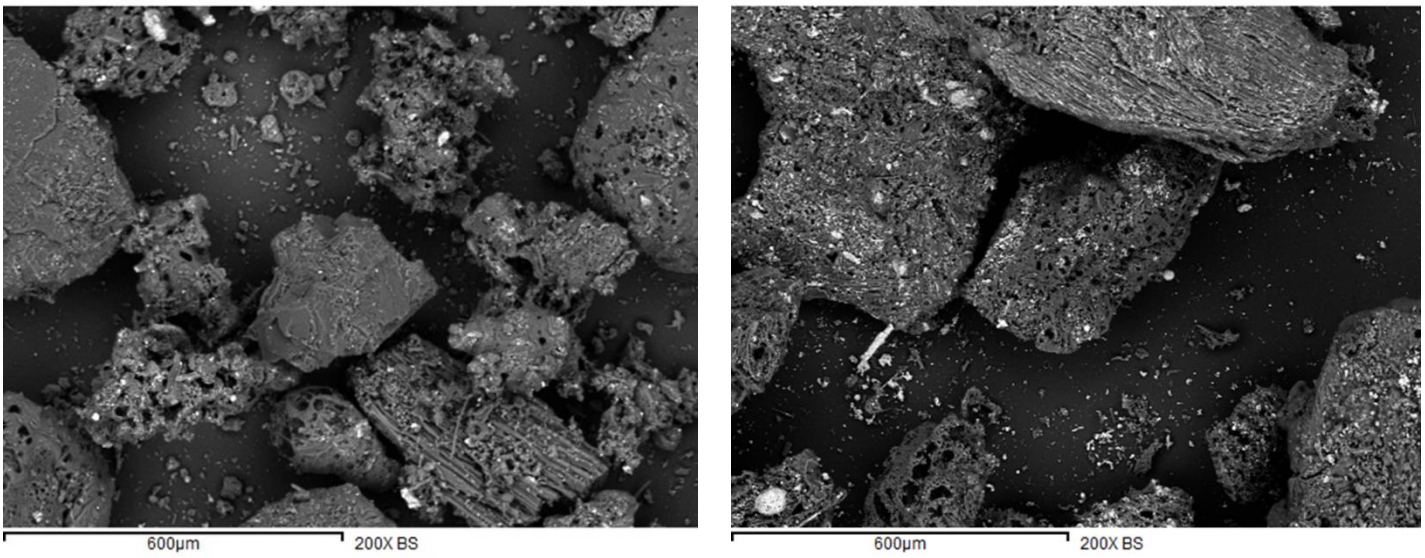

Figure 11. Backscattered images of the DTF residue of MV after a) 35ms and b) 700ms

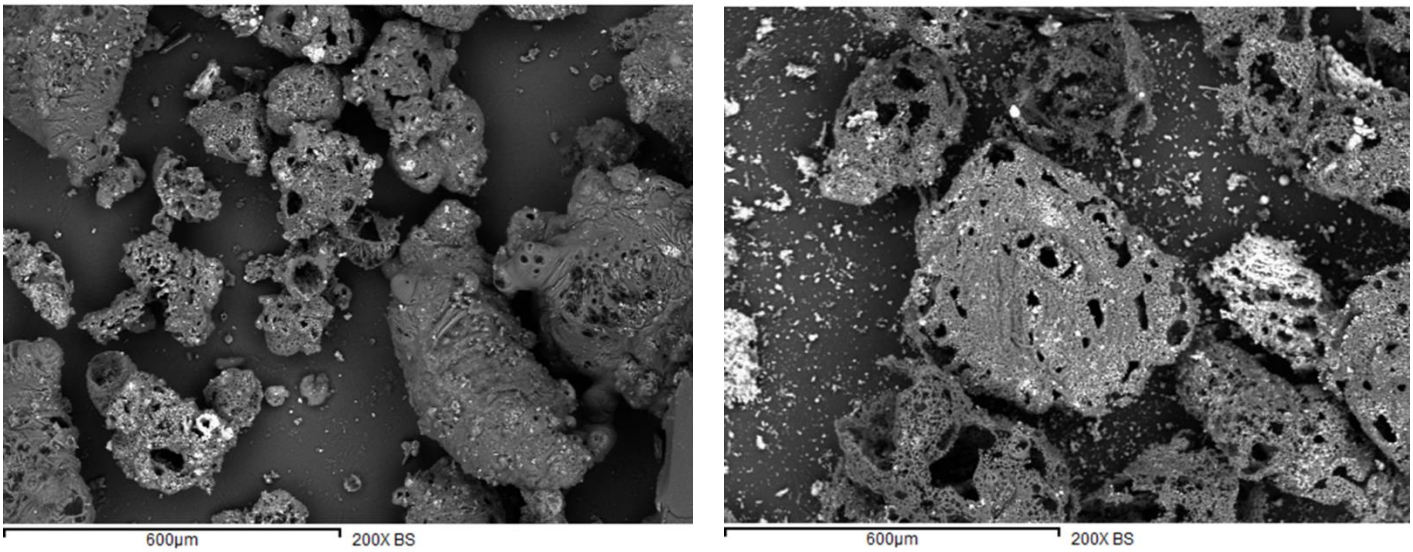

Figure 12. Backscattered images of the DTF residue of HV after a) 35ms and b) 700ms

3.5.2 Particle mineral content post DTF

It is well researched and understood that the mineral content of coals can contribute synergistic, catalytic and inhibitory effects on combustion and devolatilisation [29-34]. With this in mind, backscattered electron SEM images were collected to identify the distribution of the mineral elements. These heavier elements show up as lighter areas on the SEM images due to increased electron scattering.

The lowest burnout LV1 had larger ash particles present as discrete particles not closely associated with the char. The presence of minerals, as inclusions in the residue of the matrix, was less obvious than with the other samples, even after 700ms in the DTF. In comparison, the other low volatile coals LV2 and LV3, had more obvious mineral inclusions as flecks closely associated in the coal residue which could facilitate improved combustion compared to the LV1 and explain improved burnout compared to theoretical. The higher volatile samples also had very visible mineral inclusions in the coal residue surface at 35 ms and 700 ms in the DTF.

The other consideration with inert mineral content is that as the sample combusts the mineral concentration relative to the unburnt residue increases. This effect is most noticeable with higher volatile samples whose ash contents after a residence time of 700 ms were HV (35.2 wt%) and MV (24.4 wt%) compared to the lower volatile coals LV1 (9.4 wt%), LV2 (17.7wt%) and (LV3 14.4 wt%). A synergistic/catalytic effect by the mineral content could be a contributing reason to explain why the chars of the higher volatile coals, containing higher mineral concentrations, show good burnouts across all the residence times tested in the DTF.

In particular, the MV coal had better burnout compared to theoretical across all residence times despite a high inertinite content, which might be expected to reduce its reactivity. Coal ash samples are widely reported to contain different aluminosilicate clay mineral phases, which have been reported to produce positive combustion effects such as catalysis and negative effects such as fluxing [29-31, 33, 34, 47]. In Table 5 the elemental ratios of silicon and potassium relative to aluminium, taken from the ICP ash analysis in Table 2, indicate that MV has a higher silicon/aluminium which is likely to contribute to a reduced fluxing and a higher potassium/aluminium ratio which indicates a higher proportion of the illite mineral shown by other authors to have a synergistic/catalytic effect on burnout. There does not appear to be a correlation for all the coals but the higher potassium ratio of the MV coal and its known effect could explain the improved burnout compared to its theoretical profile and particularly on the blend with LV1 coal.

Table 5. Ash elemental ratio (normalised to LV2 ash content)

	LV1	**LV2**	**LV3**	**MV**	**HV**
Si/Al ratio	0.89	1.45	0.66	2.5	1.5
K/Al ratio	0.08	0.09	0.06	0.17	0.09
DTF burnout % (700ms)	48	59	69	74	86

4. CONCLUSIONS

The results of this work gave an insight into the blending of a semi anthracitic low volatile content coal (LV1) for granulated coal injection and the way it affects the burnout and devolatilisation with coals of different ranks and volatile content. It was found that not only was it possible to increase the burnout and volatile yield of the LV1 by blending with these other coals, but that they showed non-additive improvements relative to the theoretical values.

Even after 700ms in the DTF, the unblended higher rank LV1 showed little change in the char form and structure. In comparison, the granulated particles of the other low volatile coals showed strong fragmentation at 35ms forming cenospherical type, hollow and thin walled char structures with 'included' mineral phases which corresponded to burnout improvements. However, blending these low volatile bituminous coals could not offset the effect of increasing activation energy for the LV1 char at higher residence times (700ms) and burnouts were lower than theoretical.

Blending the highest volatile content coal and LV1 improved the low residence time burnout due to the fast release of volatile matter with some evidence of an increased particle temperature due to this, as indicated by an increased volatile yield relative to theoretical. Along with a related increase in particle swelling behaviour, and signs of a more porous char, the burnouts were correspondingly higher.

The activation energy and combustibility of the LV1 char was improved on blending with higher volatile coals and the blend with the mid volatile matter bituminous coal showed non-additive burnout improvement above theoretical at all residence times . This coal contained higher K/Al ratios associated with the mineral illite, identified in other work as contributing a synergistic or catalytic effect; along with the presence of other minerals as inclusions through the granulated coal particles, this goes some way to explaining the improved burnout. Further work would benefit from looking at the surface chemistry more closely with XPS to identify reactive or catalytic elemental associations to strengthen this conclusion.

Acknowledgement

The authorship wishes to acknowledge and thank Tata Steel Europe Ltd for financial assistance with this project and support obtaining samples.

5. REFERENCES

[1] M. Carpenter A, Use of PCI in blast furnaces, in, IEA Clean Coal Centre, 2006.

[2] S.F. Zhang, C.G. Bai, L.Y. Wen, G.B. Qiu, X.W. Lü, Gas-particle flow and combustion characteristics of pulverized coal injection in blast furnace raceway, Journal of Iron and Steel Research International, 17 (2010) 8-12.

[3] B. Guo, P. Zulli, H. Rogers, J.G. Mathieson, A. Yu, Three-dimensional simulation of flow and combustion for pulverised coal injection, ISIJ International, 45 (2005) 1272-1281.

[4] R. Maldonado, G. Hanniker, M. Pettifor, GRANULAR COAL INJECTION INTO BLAST FURNACES AT THE SCUNTHORPE WORKS OF THE BRITISH STEEL CORPORATION, in: Proceedings - Ironmaking Conference, 1985, pp. 425-435.

[5] H. Guo, B. Su, J. Zhang, J. Shao, H. Zuo, S. Ren, Energy conservation for granular coal injection into a blast furnace, JOM, 64 (2012) 1002-1010.

[6] R. Barranco, M. Colechin, M. Cloke, W. Gibb, E. Lester, The effects of pf grind quality on coal burnout in a 1 MW combustion test facility, Fuel, 85 (2006) 1111-1116.

[7] F. Li, J. Zhang, C. Qi, Q. Pang, J. Rao, C. Ma, Investigation on the dual influence of pansteel pulverized coal combustion process by coal quality and particle size, in: Materials Science and Technology Conference and Exhibition 2013, MS and T 2013, 2013, pp. 566-573.

[8] B. Yi, L. Zhang, Z. Mao, F. Huang, C. Zheng, Effect of the particle size on combustion characteristics of pulverized coal in an O2/CO2 atmosphere, Fuel Processing Technology, 128 (2014) 17-27.

[9] D. Yu, M. Xu, J. Sui, X. Liu, Y. Yu, Q. Cao, Effect of coal particle size on the proximate composition and combustion properties, Thermochimica Acta, 439 (2005) 103-109.

[10] K. Ishii, Advanced pulverised coal injection technology and blast furnace operation, Elsevier science ltd, 2000.

[11] W.H. Chen, S.W. Du, T.H. Yang, Volatile release and particle formation characteristics of injected pulverized coal in blast furnaces, Energy Conversion and Management, 48 (2007) 2025-2033.

[12] H. Li, L. Elliott, H. Rogers, P. Austin, Y. Jin, T. Wall, Reactivity study of two coal chars produced in a drop-tube furnace and a pulverized coal injection rig, Energy and Fuels, 26 (2012) 4690-4695.

[13] S. Bortz, G. Flament, EXPERIMENTS ON PULVERIZED-COAL COMBUSTION UNDER CONDITIONS SIMULATING BLAST-FURNACE ENVIRONMENTS, Ironmaking and Steelmaking, 10 (1982) 222-229.

[14] T. Suzuki, R. Hirose, K. Morimoto, T. Abe, PULVERIZED COAL COMBUSTION IN HIGH TEMPERATURE FURNACES FOR STEEL MAKING (FIRST REPORT: EVALUATION METHOD OF COMBUSTIBILITY FOR PULVERIZED COAL), Bulletin of the JSME, 27 (1984) 2803-2810.

[15] W. Kalkreuth, A.G. Borrego, D. Alvarez, R. Menendez, E. Osório, M. Ribas, A. Vilela, T.C. Alves, Exploring the possibilities of using Brazilian subbituminous coals for blast furnace pulverized fuel injection, Fuel, 84 (2005) 763-772.

[16] S. Raygan, H. Abdizadeh, A.E. Rizi, Evaluation of Four Coals for Blast Furnace Pulverized Coal Injection, Journal of Iron and Steel Research International, 17 (2010) 8-12,20.

[17] C. Moon, Y. Sung, S. Ahn, T. Kim, G. Choi, D. Kim, Thermochemical and combustion behaviors of coals of different ranks and their blends for pulverized-coal combustion, Applied Thermal Engineering, 54 (2013) 111-119.

[18] S.W. Du, W.H. Chen, J.A. Lucas, Pulverized coal burnout in blast furnace simulated by a drop tube furnace, Energy, 35 (2010) 576-581.

[19] S. Biswas, N. Choudhury, P. Sarkar, A. Mukherjee, S.G. Sahu, P. Boral, A. Choudhury, Studies on the combustion behaviour of blends of Indian coals by TGA and Drop Tube Furnace, Fuel Processing Technology, 87 (2006) 191-199.
[20] K. Kunitomo, T. Orimoto, T. Nishimura, M. Naito, J.I. Yagi, Effects of volatile matter of pulverized coal on reducing agents rate of blast furnace and combustion behavior of coal mixture, Tetsu-To-Hagane/Journal of the Iron and Steel Institute of Japan, 90 (2004) 190-197.
[21] V. Artos, A.W. Scaroni, T.g.a. and drop-tube reactor studies of the combustion of coal blends, Fuel, 72 (1993) 927-933.
[22] K.A. Davis, R.H. Hurt, N.Y.C. Yang, T.J. Headley, Evolution of char chemistry, crystallinity, and ultrafine structure during pulverized-coal combustion, Combustion and Flame, 100 (1995) 31-40.
[23] N.V. Russell, T.J. Beeley, C.K. Man, J.R. Gibbins, J. Williamson, Development of TG measurements of intrinsic char combustion reactivity for industrial and research purposes, Fuel Processing Technology, 57 (1998) 113-130.
[24] M.L. Chan, J.M. Jones, M. Pourkashanian, A. Williams, Oxidative reactivity of coal chars in relation to their structure, Fuel, 78 (1999) 1539-1552.
[25] H.K. Chagger, J.M. Jones, M. Pourkashanian, A. Williams, A. Owen, G. Fynes, Emission of volatile organic compounds from coal combustion, Fuel, 78 (1999) 1527-1538.
[26] J.M. Jones, M. Pourkashanian, C.D. Rena, A. Williams, Modelling the relationship of coal structure to char porosity, Fuel, 78 (1999) 1737-1744.
[27] L.R. Radović, P.L. Walker Jr, R.G. Jenkins, Importance of carbon active sites in the gasification of coal chars, Fuel, 62 (1983) 849-856.
[28] L. Lu, C. Kong, V. Sahajwalla, D. Harris, Char structural ordering during pyrolysis and combustion and its influence on char reactivity, Fuel, 81 (2002) 1215-1225.
[29] H. Zhang, W.X. Pu, S. Ha, Y. Li, M. Sun, The influence of included minerals on the intrinsic reactivity of chars prepared at 900 °C in a drop tube furnace and a muffle furnace, Fuel, 88 (2009) 2303-2310.
[30] J.H. Pohl, INFLUENCE OF MINERAL MATTER ON THE RATE OF COAL CHAR COMBUSTION, in: ACS Symposium Series, 1986, pp. 430-436.
[31] W. Shaolong, C. Wei-Yin, S. Guang, Roles of mineral matter in the early stages of coal combustion, Energy and Fuels, 23 (2009) 710-718.
[32] S. Gupta, Y. Al-Omari, V. Sahajwalla, D. French, Influence of carbon structure and mineral association of coals on their combustion characteristics for Pulverized Coal Injection (PCI) application, Metallurgical and Materials Transactions B: Process Metallurgy and Materials Processing Science, 37 (2006) 457-473.
[33] Z. Wei, J. Michael Moldowan, J. Dahl, T.P. Goldstein, D.M. Jarvie, The catalytic effects of minerals on the formation of diamondoids from kerogen macromolecules, Organic Geochemistry, 37 (2006) 1421-1436.
[34] R. Menendez, D. Alvarez, A.B. Fuertes, G. Hamburg, J. Vleeskens, Effects of clay minerals on char texture and combustion, Energy and Fuels, 8 (1994) 1007-1015.
[35] N. Oka, T. Murayama, H. Matsuoka, S. Yamada, T. Yamada, S. Shinozaki, M. Shibaoka, C.G. Thomas, The influence of rank and maceral composition on ignition and char burnout of pulverized coal, Fuel Processing Technology, 15 (1987) 213-224.
[36] S. Su, J.H. Pohl, D. Holcombe, J.A. Hart, Slagging propensities of blended coals, Fuel, 80 (2001) 1351-1360.
[37] J.H.W. Flynn, L.A., General Treatment of the Thermogravimetry
of Polymers, Journal of research of the national bureau of standards-A. Physics and Chemistry, 70A (1966).
[38] B.I. 11358-2:2014, Plastics-Thermogravimetry (TG) of polymers part 2: Determination of activation energy, in, 2014.
[39] J. Steer, R. Marsh, A. Griffiths, A. Malmgren, G. Riley, Biomass co-firing trials on a down-fired utility boiler, Energy Conversion and Management, 66 (2013) 285-294.

[40] T.R. Ballantyne, P.J. Ashman, P.J. Mullinger, A new method for determining the conversion of low-ash coals using synthetic ash as a tracer, Fuel, 84 (2005) 1980-1985.
[41] W.-H. Chen, S.-W. Du, C.-H. Tsai, Z.-Y. Wang, Torrefied biomasses in a drop tube furnace to evaluate their utility in blast furnaces, Bioresource Technology, 111 (2012) 433-438.
[42] E. Biagini, Marcucci, M., Review of methodologies for coal characterisation, in, International flame reserach foundation, 2010.
[43] H. Li, L. Elliott, H. Rogers, T. Wall, Comparative study on the combustion performance of coals on a pilot-scale test rig simulating blast furnace pulverized coal injection and a lab-scale drop-tube furnace, Energy and Fuels, 28 (2014) 363-368.
[44] L.A.S. Juniper, G.B, Research Achievements in Defining the Combustion Characteristics of Australian Coals in: International Coal Engineering Conference, Institution of Engineers, Australia, Sydney, 1990, pp. 129-134.
[45] C.A. Wang, Y. Liu, X. Zhang, D. Che, A study on coal properties and combustion characteristics of blended coals in northwestern China, Energy and Fuels, 25 (2011) 3634-3645.
[46] G. Liu, H. Wu, R.P. Gupta, J.A. Lucas, A.G. Tate, T.F. Wall, Modeling the fragmentation of non-uniform porous char particles during pulverized coal combustion, Fuel, 79 (2000) 627-633.
[47] D.A. Spears, Role of clay minerals in UK coal combustion, Applied Clay Science, 16 (2000) 87-95.

HIGHLIGHTS

- Blending coals improved the burnout of low volatile content semi anthracitic coals
- Granulated samples showed a fragmentation effect in a drop tube furnace
- Granulated particle fragmentation improved blend burnouts at lower residence time
- Higher volatile content mass loss improved burnout at lower residence times
- Included minerals with higher K/Al ratios gave non-additive burnout improvements